

ARTICLE

From functional genomics of vero cells to CRISPR-based genomic deletion for improved viral production rates

Marie-Angélique Sène | Yu Xia | Amine A. Kamen 

Department of Bioengineering, McGill University, Montreal, Québec, Canada

Correspondence

Amine A. Kamen, Department of Bioengineering, McGill University, McConnell Engineering Building, Room 363, 3480 Rue University, Montréal, Quebec H3A 2K6, Canada.

Email: amine.kamen@mcgill.ca

Funding information

Canada Research Chairs; Natural Sciences and Engineering Research Council of Canada

Abstract

Despite their wide use in the vaccine manufacturing field for over 40 years, one of the main limitations to recent efforts to develop Vero cells as high-throughput vaccine manufacturing platforms is the lack of understanding of virus-host interactions during infection and cell-based virus production in Vero cells. To overcome this limitation, this manuscript uses the recently generated reference genome for the Vero cell line to identify the factors at play during influenza A virus (IAV) and recombinant vesicular stomatitis virus (rVSV) infection and replication in Vero host cells. The best antiviral gene candidate for gene editing was selected using Differential Gene Expression analysis, Gene Set Enrichment Analysis and Network Topology-based Analysis. After selection of the ISG15 gene for targeted CRISPR genomic deletion, the ISG15 genomic sequence was isolated for CRISPR guide RNAs design and the guide RNAs with the highest knockout efficiency score were selected. The CRISPR experiment was then validated by confirmation of genomic deletion via PCR and further assessed via quantification of ISG15 protein levels by western blot. The gene deletion effect was assessed thereafter via quantification of virus production yield in the edited Vero cell line. A 70-fold and an 87-fold increase of total viral particles productions in ISG15^{-/-} Vero cells was achieved for, respectively, IAV and rVSV while the ratio of infectious viral particles/total viral particles also significantly increased from 0.0316 to 0.653 for IAV and from 0.0542 to 0.679 for rVSV-GFP.

KEYWORDS

functional genomics, transcriptomics, vero cells, viral vector production

1 | INTRODUCTION

Vero cells are a female African Green Monkey kidney derived cell line widely used over 40 years for viral vaccine production (Sascha Kiesslich, 2020) including the vaccine against dengue fever, influenza, Japanese encephalitis, polio, rabies, rotavirus, smallpox and more

recently, Ebola (using a recombinant vesicular stomatitis virus [VSV]) (Ammerman et al., 2008; Barrett et al., 2009; Suder et al., 2018).

The Vero cell line is part of the various cell culture-based platforms used to produce influenza vaccines to counter the drawbacks of egg-based vaccine production methods by providing a high throughput, robust and cross-contamination-free alternative.

This is an open access article under the terms of the Creative Commons Attribution-NonCommercial-NoDerivs License, which permits use and distribution in any medium, provided the original work is properly cited, the use is non-commercial and no modifications or adaptations are made.

© 2022 The Authors. *Biotechnology and Bioengineering* published by Wiley Periodicals LLC.

Nonetheless, the Vero cell line's low influenza virus production rate (Frensing et al., 2016) significantly hinders its potential for wider use.

Among the numerous approved Vero cell-based vaccines, an Ebola vaccine designed using a pseudotyped recombinant vesicular stomatitis virus (rVSV) has been shown to be safe for human administration (Agnandji et al., 2016) which further stresses the potential of rVSV as an effective vaccine production platform given the generally asymptomatic nature of VSV infections in humans (Kiesslich et al., 2020).

Furthermore, not only were Vero cells identified as the cell line with the highest susceptibility to MERS-CoV, (Liu et al., 2018) SARS-CoV and recently SARS-CoV-2, (Hoffmann et al., 2020) but also, several inactivated COVID-19 vaccines were approved and are used to immunize millions such as Sinopharm, Sinovac, CoronaVac (WHO, 2022). Thus, successful engineering of Vero cell lines to significantly increase the viral production of several viruses including influenza A virus (IAV) and rVSV would greatly impact global health.

Recent advances in gene editing made it possible to edit the genome of cell lines and notably those used for viral infection studies and vaccine production through process intensification exploiting the available genomic information. Previous attempts were made to increase viral production rates in Vero cells through gene editing using a genome-wide RNA interference screen dataset to select gene targets (Van der Sanden et al., 2016) but no significant increase in production yields was observed after repeating the study later on (Hoeksema et al., 2018). Possible reasons cited by the authors to explain such results include the use of a genome other than the Vero cell genome, and the fact that the phenotypes induced by transcriptional suppression (RNAi-based knock-down) and genetic deletion (CRISPR knockout) differ in such a way that the former increases virus production while the latter does not. Thus, it is necessary to propose a new approach that does not rely on screens to identify valuable gene targets for CRISPR/Cas9 editing.

With the availability of complete genome sequences and accurate annotations of genes and their products, the field of functional genomics has emerged as an alternative to classical molecular biology gene-by-gene-based approaches to study genes and proteins interactions and their phenotypic effects by using genome-wide methods combining genomics, epigenomics, transcriptomics, proteomics, and metabolomics among others (Bunnik & Le Roch, 2013).

With the recent publication of the Vero cell genome, (Sène et al., 2021) we hereby propose a novel approach combining the study of host-virus interactions during Vero cells infection with IAV Puerto Rico 8 and rVSV-GFP to identify gene targets and a genomic deletion method using CRISPR/Cas9 (Bauer et al., 2015) with subsequent single-cell cloning to generate an engineered cell line with high yield viral production rates.

2 | MATERIALS AND METHODS

2.1 | Cell lines and culture media

The Vero WHO cell line studied in this work was at passage 138. This cell line was derived from a vial of Vero ATCC CCL-81 which was sent to

WHO at passage 124 for analysis and establishment of the Vero WHO master cell bank approved for vaccine production. The cells were grown in static culture at 37°C and 5% CO₂ in a humidified incubator (Infors HT). Cells were passaged twice weekly using TrypLE Express (Thermo Fisher Scientific) as a dissociation reagent. A serum-free adapted sub-cell line grown in OptiPRO medium (Thermo Fisher Scientific) supplemented with 4 mM GlutaMAX (Thermo Fisher Scientific) was cryopreserved at a passage number of 151 in OptiPRO medium supplemented with 4 mM GlutaMAX and 10% dimethyl sulfoxide (Sigma).

A quality control kinetics experiment was run in which Vero cells were infected with IAV Puerto Rico 8 strain and rVSV-GFP at multiplicity of infection (MOI) 10 to quantify the viral production rate and the cell viability over time. That led to the identification of the best time window to harvest samples for RNA sequencing (highest viability and before induction of cell death to avoid having false enrichment of the cell death-related pathways).

The supernatant was harvested at several time points and cell viability was monitored. To quantify the virus production for each time point, TCID₅₀ (The median tissue culture infectious dose 50%) and hemagglutination assay were used.

Following the kinetics analysis, for transcriptome analysis, Vero WHO cells at passage 153 were infected with IAV Puerto Rico 8, rVSV-GFP and harvested before visible cytopathic effect at 24 and 6 hpi, respectively. Due to the nature of rVSV infection which makes the cytopathic effect clearly visible at the microscope at early stages, monitoring of cell viability was done using the microscope. The viability was assessed using a cell counter for the IAV, since the cells are able to withstand infection at MOI 10 for more than 48 h without visible cytopathic effects. The samples were harvested using TrypLE Express and centrifuged at 300g for 5 min. Cell pellets of around 6 million cells were lysed and quickly frozen in a mixture of dry ice/ethanol and stored at -80°C until further analysis, samples made of noninfected cells were also prepared and sent to sequencing as control batch. All the samples were generated in triplicates.

2.2 | Differential gene expression analysis

Total RNA sequencing (TrueSeq) was performed using Illumina NovaSeq6000 Sprime v1.5, PE100. Following standard quality control, the reads were first aligned to the recently published Vero cell genome (Sène et al., 2021) using STAR (Dobin et al., 2013) and the resulting BAM files were sorted by name using SAMtools (Li et al., 2009) before read count. Transcripts were quantified using featureCounts (Liao et al., 2014). Differential expression analysis of the raw read counts was done using DESeq2 (Love et al., 2014). The resulting differentially expressed (DE) gene list was filtered with a *p* value cut-off of 0.0001 (Tables S1 and S2).

2.3 | Downstream analysis of DE genes

The DE genes were ranked based on their log₂ fold change.

WebGestalt (WEB-based GENE SeT AnaLysis Toolkit) (Liao et al., 2019) was used for gene set enrichment analysis (GSEA) with the Reactome gene set collection. To find DE pathways of genes between noninfected and infected cells, gene sets were filtered and the top 20 gene sets with an adjusted p value lower than 0.05 were considered as significantly changed.

The upregulated part of the gene list generated by DESeq2 was filtered to consider genes with a $|\log_2$ fold change > 2 for Network Topology Analysis (NTA) based on the Network Retrieval & Prioritization construction method (Wang et al., 2017) by first using random walk analysis to calculate random walk probability for the input gene IDs (seeds), then identifying the relationships among the seeds in the selected network to return a retrieval subnetwork where the top 20 genes with the top random walk probability are highlighted. Indeed, assuming a tight connection between mechanistically important genes and a random distribution of other genes on the network, the Network Topology-based Analysis (NTA) uses random walk-based network propagation by identifying those genes which are potentially biologically significant. Our input gene IDs (upregulated genes previously filtered) were used as seeds, and based on their overall proximity (quantified by the random walk similarity) to the input seeds, each gene in the protein-protein interaction (PPI) network was attributed a score. Then, the statistical significance of those scores was calculated via two p values: a global p value whose significance is the result of a nonrandom association between the gene in the PPI network and the input seeds; and a local p value whose significance ensures that the gene did not acquire a significant association with the input seeds simply because of network topology.

Finally, enrichment analysis of the retrieved subnetworks was done using the PPI BIOGRID (Stark et al., 2006) database and Gene Ontology (GO) Biology Process terms (Harris et al., 2004). The GO terms were first ranked based on their adjusted p value and only the top 10 highly significant terms with an adjusted p value cut-off of 0.01 were considered.

2.4 | SG15 protein sequences comparison

ISG15 protein sequences were retrieved from RefSeq for Vero cells (XP_007979280.1), human (NP_005092.1), mice (NP_056598.2) and canine (XP_003639101.1). The sequences were aligned using T-Coffee (Di Tommaso et al., 2011) and exported to the ESPrInt server (Robert & Gouet, 2014) for sequence alignment graphic design. Regions known to interact with viruses are also highlighted.

2.5 | Genomic deletion using CRISPR/Cas9

The strategy used for this genomic deletion protocol relies on cellular delivery of a pair of chimeric single guide RNAs (sgRNAs) to create two double-strand breaks at a locus to delete the intervening DNA segment by nonhomologous end joining (NHEJ) repair. This method has been used to delete genes with a length between 1 and 10 kb (Bauer

et al., 2015) and is being applied here for the deletion of the genes' CDS regions. Genomic deletions are more advantageous compared to HDR or single-site small indel production because not only does the high frequency of deletions limit the number of clones needed to be screened to find clones of interest, and monoallelic and biallelic deletions can be easily identified via PCR avoiding labor intensive methods. But also, given that a significant portion of the gene of interest is deleted, reliable loss-of-function alleles can be obtained.

A pair of guide RNAs was designed using freely available online tools CRISPOR (Concordet & Haeussler, 2018) and EuPaGDT (Peng & Tarleton, 2015) which already included the Vero cell genome in their list of custom genomes. These tools helped identify guide sequences that minimize identical genomic matches or near-matches to reduce the risk of cleavage away from target sites (off-target effects). The guide sequences consist of a 20-mer ("protospacer sequence") upstream of an "NGG" sequence ("protospacer adjacent motif" or PAM) at the genomic recognition site. The plasmid structures pX458 (Addgene plasmid ID 48138) containing our designed gRNAs (guide A: ACCAGCATTCGAG CAAGATCAAGG; guide B: GGAAACCGAAACTTGCCACCGG), which include GFP as a selectable marker, were purchased from GenScript.

The delivery of CRISPR/Cas9 plasmids was done by electroporation. Four vials containing 2.6×10^6 cells in 90 μ l of growth medium were prepared for transfection. The cells were washed two times in ice-cold phosphate-buffered saline, resuspended and transferred to a 4-mm gapped cuvette. Four tubes of 10 ml growth media were prepared and put into the incubator for 10 min. A total of 5 μ g of each CRISPR/Cas9 construct A and B were mixed with the Vero cell suspensions and the samples were immediately pulsed using an electroporator at 250 volts square wave for 20 ms. The cells were then diluted into the previously prepared 10 ml prewarmed complete growth media and plated in a T75 cm (Barrett et al., 2009) flask before incubation at 37°C, 5% CO₂ for 48 h. For all studies, nontransfected cells were included as a negative control.

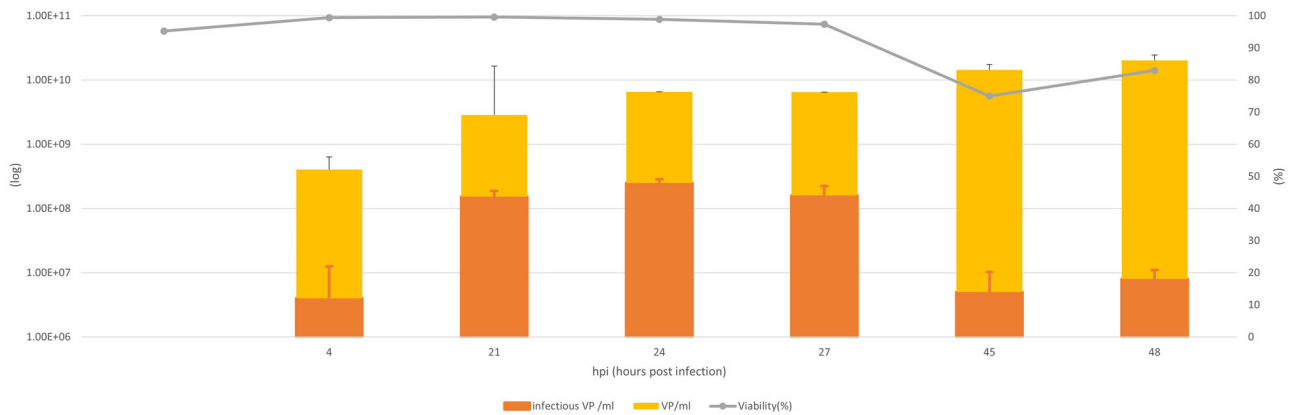
2.6 | FACS sorting, single-cell cloning, and gene editing validation

The top approximately 3% of GFP positive cells were sorted using FACS to enrich for cells that received high levels of the CRISPR/Cas9 constructs. The sorted cells were individually plated into 96-well plates containing 100 μ l per well of cell culture media using FACS sorter. The clones were incubated at 37°C for 3 weeks. The resulting monoclonal colonies were passaged and split to proceed with validation steps.

PCR was used to validate the intended genomic deletion of the ISG15 CDS region. One set of primers lying internally of the sequence to be deleted (nondeletion band: if a band is generated from this pair of primers then the deletion did not occur) and another set of primers upstream and downstream of the sgRNA cleavage sites (deletion band: if a band is generated from this pair of primers then the deletion did occur) were designed (Figure 6 and Table 1). In the absence of deletion, the deletion band is often too large to efficiently amplify. Primers at least 100 bp separated from the predicted cleavage site were used to ensure

TABLE 1 Primers designed for genomic deletion of ISG15 validation

Band to be detected	Forward primer	Reverse primer
Nondeletion band	GTCCCAGCTCTGCAGACATTA	GAGCTCGGCCAGGTTCTAAG
Deletion band	CCTCGAGGCTGTAAGTCAAA	ACCATAGGGGTGTTTTCCGT

**FIGURE 1** Kinetics of IAV PR8 production in Vero cells. Quantification of both viral particles (VP/ml in orange) using ddPCR and infectious particles (TCID₅₀/ml in yellow) using TCID₅₀ and monitoring of cells viability (% in gray). IAV, influenza A virus

detection would not be impacted by a small indel at the sgRNA target site. The genomic DNA was extracted from each clone using Invitrogen PureLink Genomic DNA Mini Kit and DNA concentration was measured. Each clone was screened for both nondeletion band and deletion band detection using the following PCR protocol: for each detection, a 25 μ l PCR reaction containing 12.5 μ l master mix, 0.5 μ l forward primer (10 μ M), 0.5 μ l reverse primer (10 μ M), 100 ng gDNA, and H₂O up to 25 μ l was run in the thermocycler (98°C for 30 s, 35 cycles of (98°C for 10 s, 60°C for 30 s, 72°C for 1 min), and 72°C for 2 min). The PCR products were then run on 2% agarose gel at 10 V/cm using 1x tris-acetate-EDTA (TAE) buffer. The samples were examined for the detection of nondeletion and deletion bands using a Chemidoc (Biorad) (Figure S1) and clones with biallelic deletions were passaged and split for cell banking and further validation analysis. This validation was repeated at a week's interval for quality control. Six independent clones with biallelic deletions were used for the remaining validation steps.

Following the validation of the intended genomic deletion of the ISG15 CDS region, validation at the protein level was done via western blot to ensure that the ISG15 protein is indeed deleted (Figure S2). A total of 20 μ l of each cell lysate sample were mixed with SDS loading buffer, separated on SDS-PAGE gels (BioRad Criterion TGX Precast gels), and transferred to polyvinylidene difluoride membranes. Immunoblotting was performed using the relevant antibodies (anti-ISG15; Invitrogen). Horseradish peroxidase coupled secondary antibodies were detected with the BioRad Clarity Western ECL substrate. The resulting signals were imaged with a Chemidoc (BioRad) and analyzed by ImageJ.

Following the confirmation of ISG15 deletion, the next validation step consisted of verifying the phenotypic impact of such deletion on virus reproduction. Therefore, triplicates of wild-type Vero cells and

ISG15^{-/-} Vero cells were cultured and infected at MOI 10 with, on one hand, IAV PR8 and on the other hand rVSV-GFP. The supernatant for each sample was harvested 24 h postinfection and virus production was quantified via ddPCR (viral genome to quantify the total number of particles) and TCID₅₀ (to quantify the number of infectious viral particles) as previously described (Dzimianski et al., 2019). We ensure that the cell concentration would not influence the comparison between control and ISG15^{-/-} Vero cells by using the same cell concentrations for both cases and for all triplicates.

3 | RESULTS

3.1 | Preliminary kinetics study

The optimal harvesting time point for RNA sequencing was selected based on the infectious viral particles production level and the viability of the cells. Thus, for IAV (Figure 1), the selected time points were at the peak of infectious viral particles production (i.e., 24 hpi). For rVSV-GFP (Figure 2), given the observation of significant cytopathic effects at the initial stages (8 hpi), the time point selected was 6 hpi to ensure that pathways such as cell death are not falsely enriched simply due to sampling quality issues.

3.2 | Functional genomics analysis and gene target selection

Following the DESeq2 (Love et al., 2014) DE analysis and an applied *p* value cut-off of 0.0001, GSEA using Reactome (Fulber et al., 2021) as a

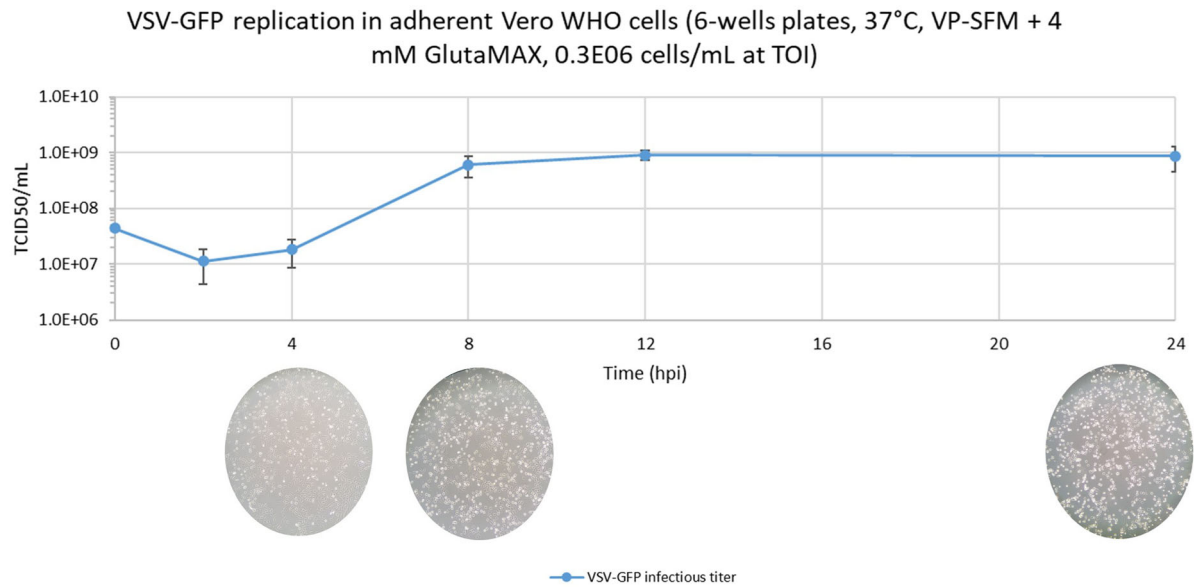


FIGURE 2 Kinetics of rVSV-GFP production in Vero cells. Quantification of infectious particles (TCID₅₀/mL in blue) using TCID₅₀ and monitoring of cytopathic effects (cell viability) via microscope. rVSV, recombinant vesicular stomatitis virus

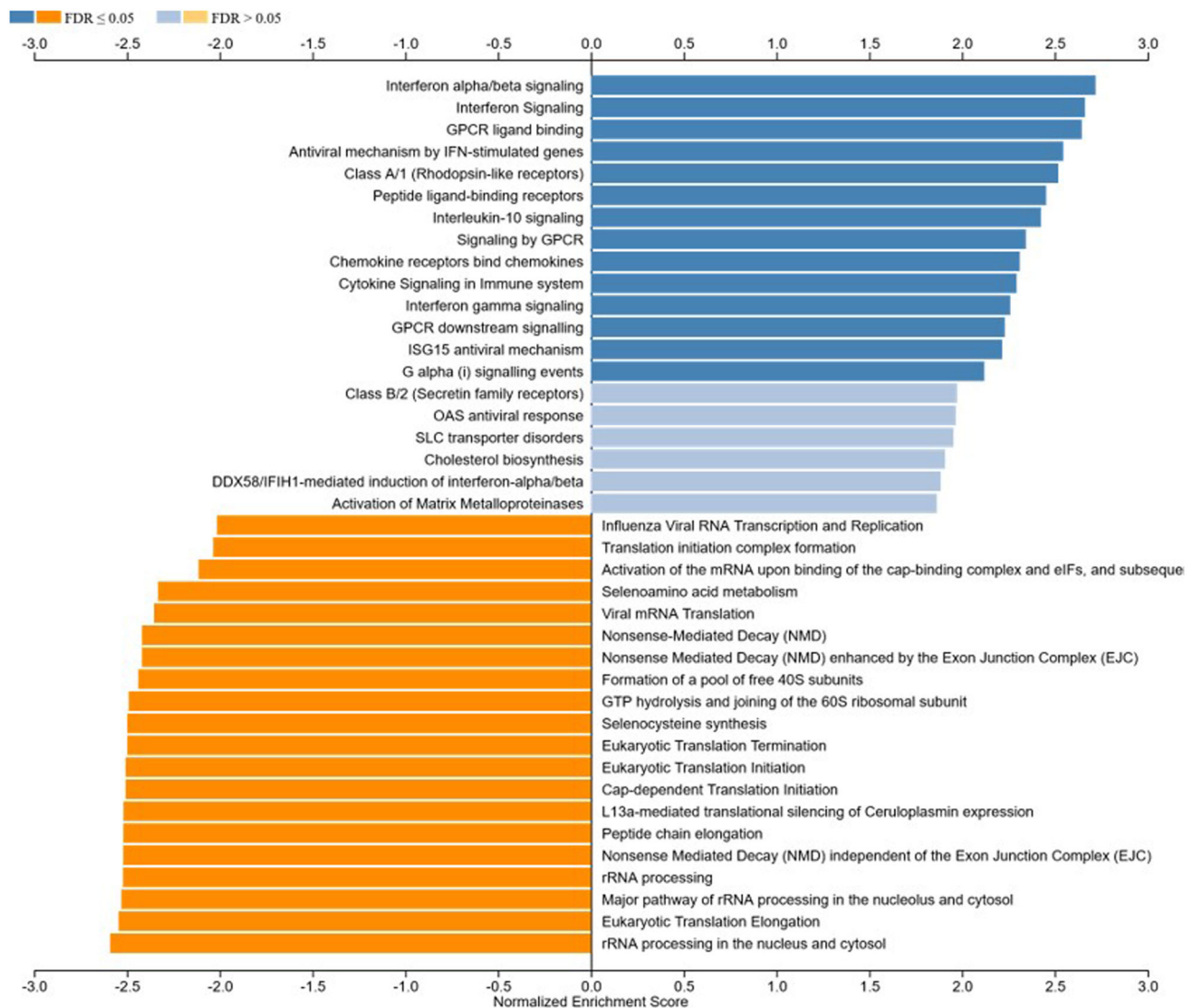


FIGURE 3 GSEA bar chart with significantly enriched hallmark pathways for 24 hpi Influenza virus infection highlighted (FDR < 0.05). FDR, false discovery rate; GSEA, gene set enrichment analysis

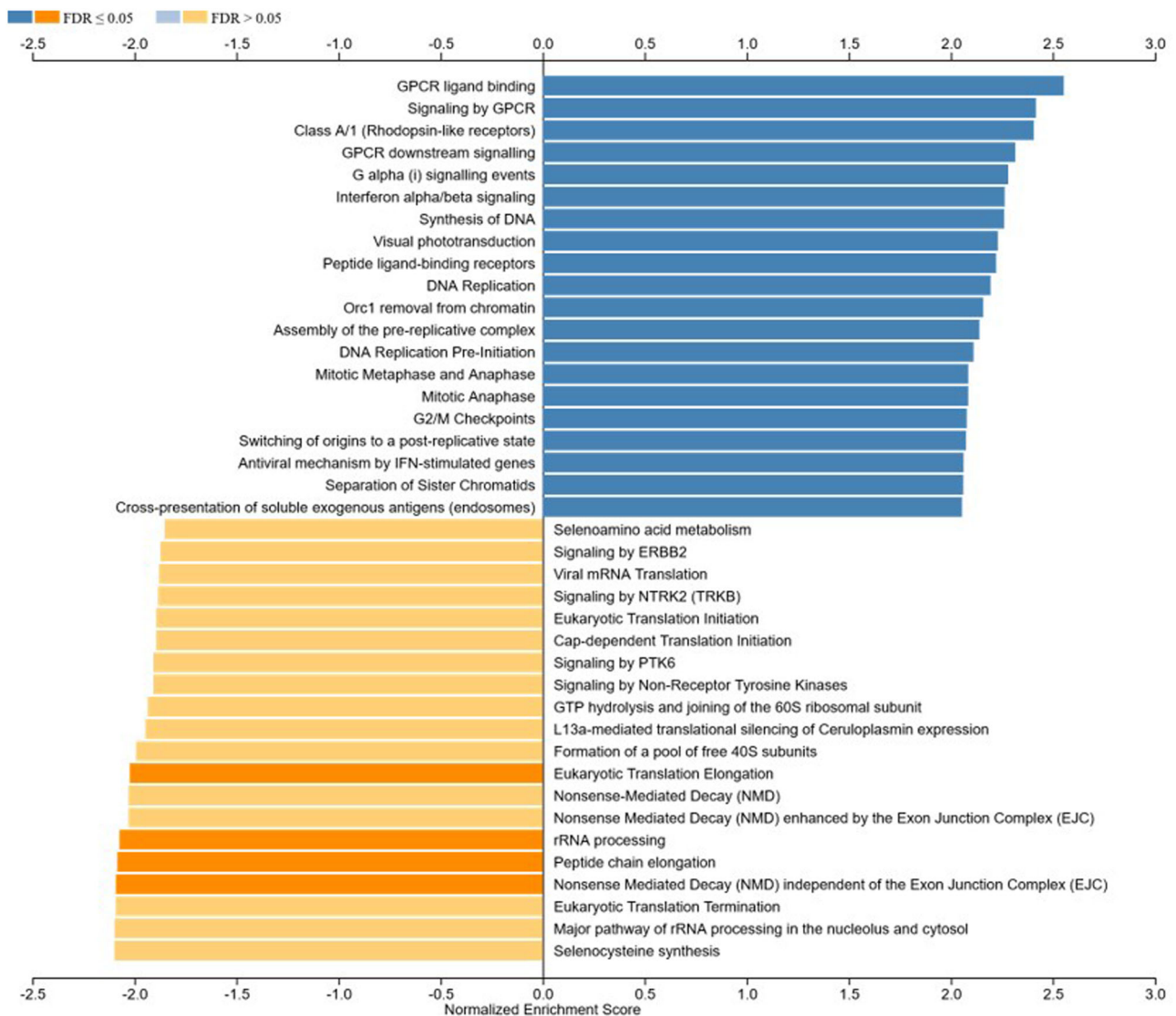


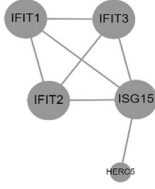
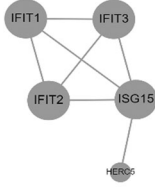
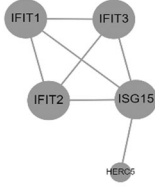
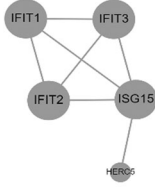
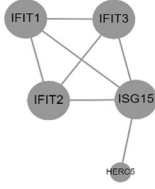


FIGURE 4 GSEA bar chart with significantly enriched hallmark pathways for 6 hpi VSV-GFP virus infection highlighted (FDR < 0.05). FDR, false discovery rate; GSEA, gene set enrichment analysis; VSV, vesicular stomatitis virus

gene set showed the following results. In the case of IAV infection at 24 hpi (Figure 3), a downregulation of major RNA processing gene sets such as the Influenza viral RNA transcription and replication gene set, the activation of messenger RNA upon binding of the cap-binding complex and eIFs and L13a-mediated translational silencing of Ceruloplasmin expression which correlates with viruses evasion strategies via cap snatching and the host cell's attempts to counter that evasion (normal enrichment scores of -2, -2.2, and -2.5 respectively). On the other hand, selenium related pathways are also downregulated such as selenoamino acid metabolism and selenocysteine synthesis. Indeed, it was previously shown that selenium and selenoproteins deficiency leads to increased host susceptibility to viral infection (Croft et al., 2014). Meanwhile, key immune response related pathways are significantly upregulated such as interferon signaling, cytokine signaling and chemokine signaling. More precisely, an upregulation of interferon (IFN)-stimulated genes and ISG15 antiviral mechanism are upregulated. Similar to IAV, rVSV-GFP interaction

with Vero cells at 6 hpi showed downregulation of one of the key quality control mechanisms of RNA processing: the nonsense mediated decay (Guillin et al., 2019) (normal enrichment score: -2.5) thus promoting viral reproduction alongside the downregulation of eukaryotic translation elongation (normal enrichment score: -2.6) (Figure 4). Moreover, the previously identified antiviral pathways related to interferons are also upregulated in the case of rVSV-GFP infection, notably, the antiviral mechanism by IFN-stimulated genes such as ISG15.

To go beyond gene sets and pathways and identify key antiviral genes involved in PPI networks, a NTA was performed for the previously identified significantly upregulated genes (264 genes for IAV 24 hpi and 235 for rVSV-GFP 6 hpi). For in both cases (Tables 2-3), in any of the pathways identified such as defense response, viral life cycle, response to cytokine, interferons, negative regulation of viral genome regulation among others, ISG15 plays a central role thus emerging as an attractive candidate for knockout via CRISPR/Cas9.

TABLE 2 Key upregulated networks and their top associated genes for rVSV-GFP infection 6 hpi (NTA: the top 10 highly significant networks with an adjusted *p* value cut-off of 0.01)

Subnetwork layout	Pathway GO ID	Pathway GO name	Top ranking associated genes
	GO:0006952	Defense response	ISG15, IFIT1, IFIT2, IFIT3, HERC5, CCL2, CCL5, CXCL8, FOS, CYP19A1
	GO:0009615	Response to virus	ISG15, IFIT1, CCL2, CCL5, CXCL8
	GO:0019079	Viral genome replication	ISG15, IFIT1, CCL2, CCL5, CXCL8
	GO:0034097	Response to cytokine	ISG15, IFIT1, IFIT2, IFIT3, CCL2, CCL5, CXCL8, FOS, TRAF1
	GO:0034340	Response to type I interferon	ISG15, IFIT1, IFIT2, IFIT3
	GO:0045069	Regulation of viral genome replication	ISG15, IFIT1, CCL5, CXCL8
	GO:0051607	Defense response to virus	ISG15, IFIT1, IFIT2, IFIT3, HERC5

Note: ISG15 is present in each network with *p* value >0.01 (nodes sizes are proportional to gene's significance).

Abbreviations: NTA, Network Topology Analysis; rVSV, vesicular stomatitis virus.

Indeed, following these results, literature search showed that ISG15 is a 17 kDa antiviral protein (15 kDa after maturation; Popp et al., 2020) that protects the host via the inhibition of viral replication in a conjugation-dependent manner and is implicated in antiviral responses to various viruses such as SARS-CoV, Influenza virus, HIV, Hepatitis virus among others.

By conjugating host and viral proteins via ISGylation, ISG15 was reported to enhance pathogenesis, inhibit nuclear translocation, budding and release of viral particles, impede viral RNA synthesis and viral protein translation, decrease infectivity of produced viral particles and suppress viral growth (Perng & Lenschow, 2018).

A functional diversity across species was also previously reported with ISG15-deficient patients showing no increased viral yield following viral infection compared to ISG15-deficient mice. Thus, looking further into that diversity especially for Vero cells to ensure that gene editing of ISG15 will lead to phenotypic modifications with regards to viral infection, the ISG15 protein sequences were compared between species of interest in the context of vaccine production (Figure 5). Protein sequence modifications between human ISG15 and murine ISG15 were like those between human ISG15 and Vero ISG15, especially at position 89 which was previously highlighted as a key player in the ability of Old-World Monkey ISG15 (including Vero cells) to more efficiently ISGylate proteins compared to human ISG15 (Pattyn et al., 2008) thus, giving some indications concerning the desired effects of ISG15 deletion in Vero cells by sowing the similarity with murine ISG15 which showed a 20-fold increase after knockout.

3.3 | ISG15 deletion validation at the genomic/proteomic level and virus production quantification

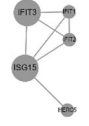





Following CRISPR/Cas9-based genomic deletion of ISG15 CDS region, several validation steps were designed to confirm plasmid delivery using a GFP reporter and cell sorting, intended deletion using PCR, protein deletion using western blot and deletion of phenotypic effects via viral infection and virus production quantification.

To confirm the genomic deletion, two pairs of PCR primers were designed (Figure 6) (one pair inside the deletion region and one outside) to screen for deletion band and nondeletion band (Figure 7) and among the 100 clones plated, 38 clones were isolated with a growth rate similar to parental Vero and 6 were identified with a biallelic deletion and good fitness (via monitoring of the clones doubling time).

At the protein level, western blot showed that none of the previously selected clones had a band at 15–17 kDa which was visible in parental or wild type Vero cells.

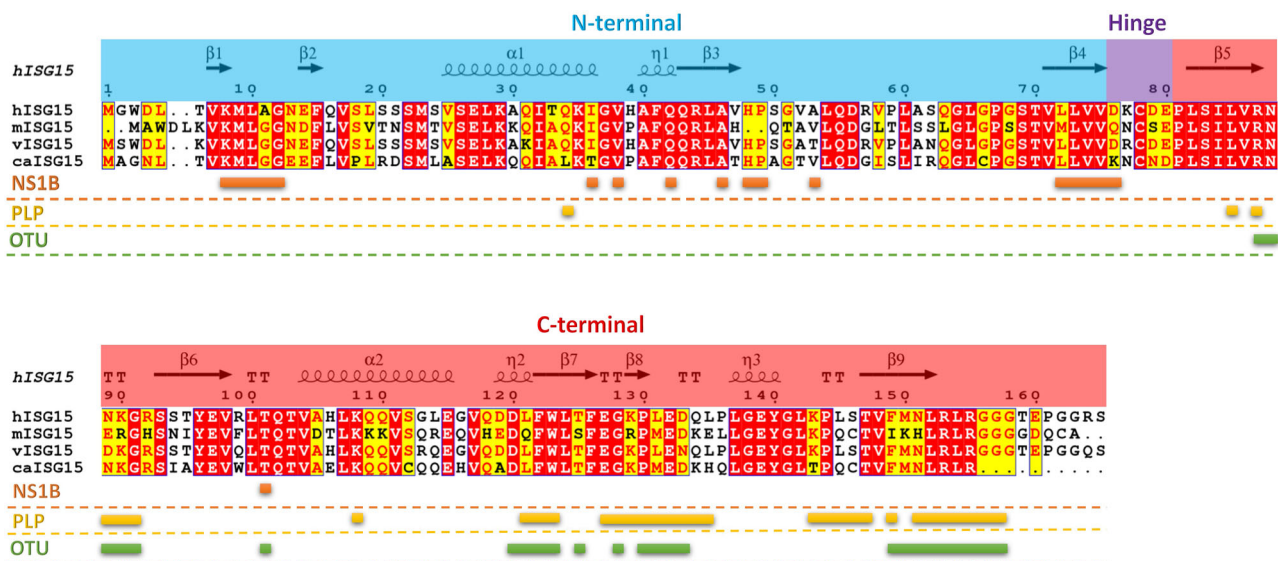
Infection of the engineered clone (Figure 8) showed a significant increase not only in total viral particle production but also in infectious viral particles. Indeed, an increase of 70.3-fold of total viral particles was observed for IAV infection and an increase of 87-fold was shown for rVSV-GFP. Interestingly, the ratio of infectious viral particles/total viral particles also significantly increased from 0.0316 to 0.653 for IAV and from 0.0542 to 0.679 for rVSV-GFP.

TABLE 3 Key upregulated networks and their top associated genes for IVA PR8 infection 24 hpi (NTA: the top 10 highly significant networks with an adjusted *p* value cut-off of 0.01)

Subnetwork layout	Pathway GO ID	Pathway GO name	Top ranking associated genes
	GO:0009615	Response to virus	CCL5, ISG15, IFIT1, IFIT2, IFIT3, HERC5
	GO:0019079	Viral genome replication	CCL2, CCL5, ISG15, IFIT1
	GO:0034340	Response to type I interferon	ISG15, IFIT1, IFIT2, IFIT3
	GO:0045071	Negative regulation of viral genome replication	CCL5, ISG15, IFIT1
	GO:0051607	Defense response to virus	ISG15, IFIT1, IFIT2, IFIT3, HERC5
	GO:0071345	Cellular response to cytokine stimulus	CCL2, CCL5, ISG15, IFIT1, IFIT2, IFIT3, TRAF1, SFRP1, PTGS2

Note: ISG15 is present in each network with *p* value >0.01 (nodes sizes are proportional to gene's significance).

Abbreviations: IVA, influenza A virus; NTA, Network Topology Analysis.

**FIGURE 5** Comparison of ISG15 protein sequences across species and Vero cells. A sequence alignment of human ISG15 (hISG15), mouse ISG15 (mISG15), vero ISG15 (vISG15) canine ISG15 (caISG15). The residues of ISG15 known to interact with the influenza virus NS1 protein, coronavirus PLPs, and nairovirus OTUs are indicated (Adli, 2018)

4 | DISCUSSION

In this work, we present a detailed analysis of virus-host interactions during IAV and rVSV-GFP infection of Vero cells to better understand the dynamics taking place between the host attempting to minimize the impact of viral infection and the viruses

attempting to evade host immune responses. Using a novel approach combining functional genomics and cell biology, we propose a new strategy for a more efficient targeted CRISPR (Adli, 2018) gene editing. Opening new possibilities for Vero cells' establishment as a pandemic-ready high throughput vaccine production platform.

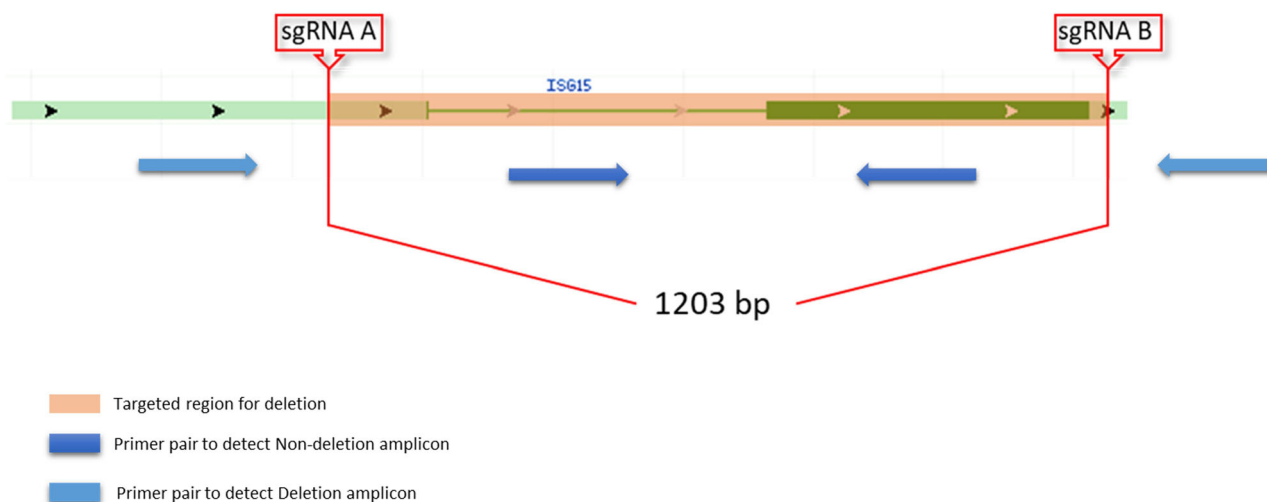


FIGURE 6 PCR primers design. For the detection of nondeletion and deletion bands

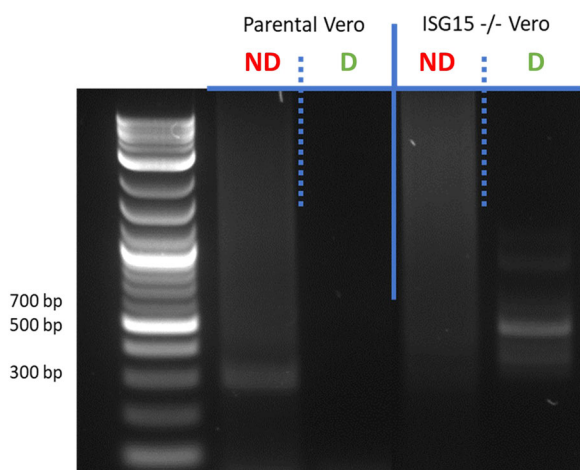


FIGURE 7 PCR Screening of clones with biallelic deletions of ISG15 CDS region. Biallelic clones selected based on the absence of nondeletion band (expected size 304 bp) and the presence of deletion band (expected size around 500 bp)

Indeed, previous attempts to generate engineered cell lines for high yield virus production relied mainly on screening data to choose gene targets followed by knocking them out via CRISPR to verify that the previously reported viral production yield in the screening data is achieved (Orr-Burks et al., 2019; Van der Sanden et al., 2016). However, in most cases, the knockout did not result in a significant increase in virus production due to several factors. These factors include: (i) knock-down and knockout do not lead to the same phenotypic effects; (ii) up to four different guide RNAs are used for screening raising the possibility of off-target effects that could lead to increased yields in virus production in unknown ways; and (iii) another genome or cell line was used for screening compared to the actual cell line used for targeted gene editing. With the recent

publication of the de novo assembled and annotated Vero genome (Sène et al., 2021) and the use of functional genomics, we were able to better understand the mechanisms involved in infection and the gene target candidates before selection, allowing us to better control and monitor the gene editing experiment.

Notably, the deletion of a whole genomic region, (Bauer et al., 2015) here the CDS region, was preferred over a sgRNA-based cut to increase the probability of getting a biallelic deletion. That way, we could ensure that the deletion will lead to the desired loss of function of the targeted gene product but also to make the validation step easier thus, ensuring a rapid and high throughput gene-editing protocol.

Interestingly, our deletion of ISG15 in Vero cells led to, alongside the overall increase in total particles production to up to 87-fold, an increase of infectious particles production ratio from 3.2% to 65.3% for IAV and from 5.4% to 67.9% for rVSV-GFP, which confirm previous report that ISG15 modulates the released infectious particles ratio while intracellular viral replication remains intact (Stark et al., 2006). In addition, during the preliminary study of IAV infection kinetics, it was shown that infectious particles production increases until 24 hpi before decreasing dramatically (Figure 1), which was also observed during influenza virus infection in HEK-293 and MDCK cells (Speer et al., 2016). Thus, this newly engineered cell line could present even more attractive advantages particularly to produce live vaccines. Therefore, as future work, it would be interesting to study the kinetics of IAV infection in the engineered ISG15^{-/-} Vero cell line to monitor the effects of ISG15 deletion on infectious particles release especially after 24 hpi. Nevertheless, it is important to point out that while ISG15 is a valuable candidate for gene editing in cell lines used for vaccine production, the protein sequence differences of ISG15 in different species should be treated with caution. Indeed, ISG15 knockout showed no effects in human cells when it comes to viral yield while showing increased viral production yield in mice and

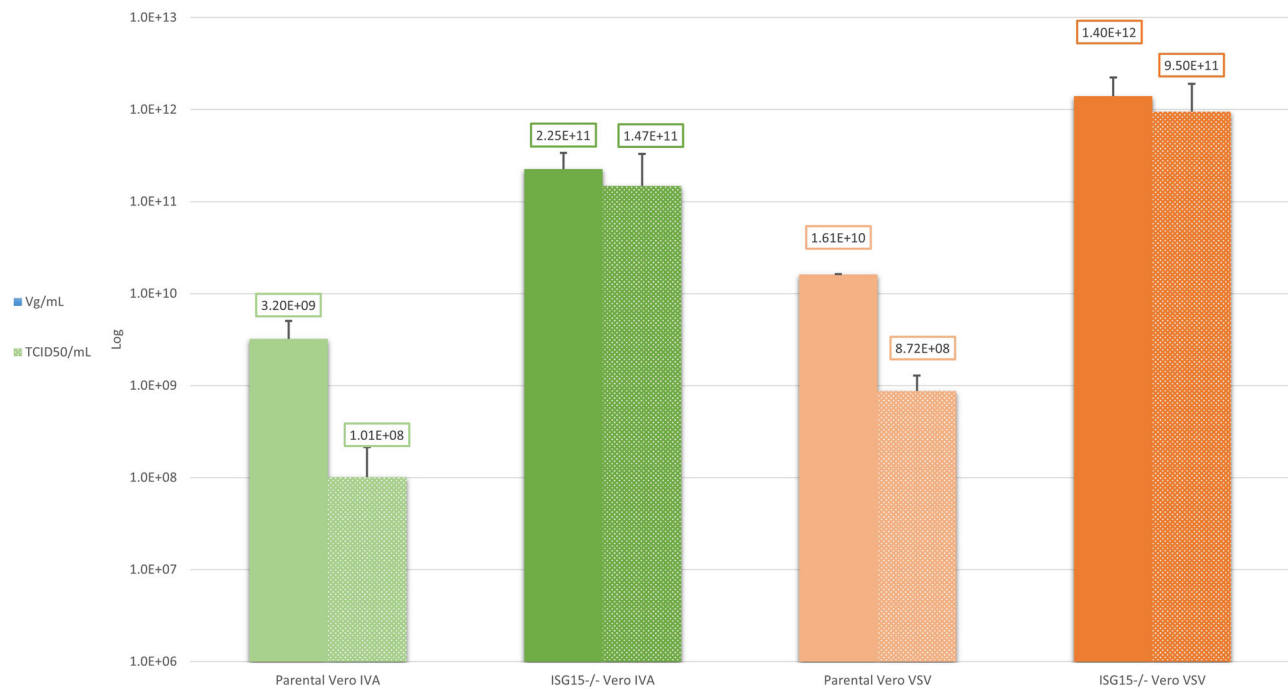


FIGURE 8 Effect of ISG15 deletion on Virus production rate. Quantification of parental Vero and ISG15^{-/-} Vero cells IAV and rVSV-GFP viral genomes and infectious particles production (Vg: Viral genome). IVA, influenza A virus; rVSV, vesicular stomatitis virus

Vero cells for instance. Thus, in the case of HEK293 cells, given that they are derived from human cells, before applying the ISG15 deletion protocol presented in this paper to HEK293 cells, it is necessary to at least investigate the ISG15 protein sequence of HEK293 to verify the mutations and their similarity with mice and Vero cells to have a rough idea of the possible effects of ISG15 deletion in HEK293 cells. Similarly, MDCK cells being derived from canine, the corresponding protein sequence was also compared to the ISG15 protein from Vero cell, mice and human with key mutation located at sites known to interact with viruses (Figure 5) which increases the chances of successful gene knockout. But again, as shown with Vero cells which present significant differences with the African Green Monkey genome, (Sène et al., 2021) it is important to verify that, indeed, the MDCK ISG15 protein sequence is like *Canis lupus familiaris* ISG15 at least in the regions known to interact with viruses.

Based on NTA data, alongside ISG15, other promising candidates were also highlighted: IFIT1 and CCL5 for instance. These could be attractive candidates for multiple gene deletions alongside ISG15 but given the lack of data for these targets compared to ISG15, it is recommended to first study them beforehand and do incremented deletions to have a better prediction on the possible effects that could affect cell fitness and whether or not an additional increase or synergistic viral yield could be observed.

Overall, the Vero cell line was one of the first cell lines considered as a vaccine production platform with various vaccines produced in Vero cells being approved and used to immunize large populations including in the current COVID-19 pandemic. With this new approach, we successfully engineered a cell line capable of increasing virus production yield to up to 87-fold while also increasing infectious viral particles

release that was around 3.2%–5.4% to up to 65.3%–67.9%. Thus, the key findings of this study open new avenues for the development of pandemic-ready vaccine production platforms in line with the global preparedness plan.

AUTHOR CONTRIBUTIONS

Marie-Angélique Sène: designed all experiments, executed all experiments, and prepared the manuscript. **Yu Xia and Amine A. Kamen:** provided guidance, supervision, and critical reading of the manuscript.

ACKNOWLEDGMENTS

This work was supported by funding from the Natural Sciences and Engineering Research Council (NSERC-Grant-CRDPJ 511957). M-A-S is supported by the McGill Engineering Doctoral Award (MEDA) and A.A.K by a Canada Research Chair (CRC-240394).

The authors would like to thank Denis Flipo (UQAM) for assistance with FACS sorting and Shantoshini Dash (McGill University) for performing the western blot.

CONFLICTS OF INTEREST

The authors declare no conflicts of interest.

DATA AVAILABILITY STATEMENT

Raw RNA reads are available under the bioproject PRJNA644395. All other relevant data are available upon request.

ORCID

Amine A. Kamen  <http://orcid.org/0000-0001-9110-8815>

REFERENCES

- Adli, M. (2018). The CRISPR tool kit for genome editing and beyond. *Nature Communications*, 9, 1911.
- Agnandji, S. T., Huttner, A., Zinser, M. E., Njuguna, P., Dahlke, C., Fernandes, J. F., Yerly, S., Dayer, J. A., Kraehling, V., Kasonta, R., Adegnika, A. A., Altfeld, M., Auderset, F., Bache, E. B., Biedenkopf, N., Borregaard, S., Brosnahan, J. S., Burrow, R., Combescure, C., ... Siegrist, C.-A. (2016). Phase 1 trials of rVSV Ebola vaccine in Africa and Europe. *New England Journal of Medicine*, 374(17), 1647–1660. <https://doi.org/10.1056/NEJMoa1502924>
- Ammerman, N. C., Beier-Sexton, M., & Azad, A. F. (2008). Growth and maintenance of Vero cell lines. *Current Protocols in Microbiology*. <https://doi.org/10.1002/9780471729259.mca04es11>
- Barrett, P. N., Mundt, W., Kistner, O., & Howard, M. K. (2009). Vero cell platform in vaccine production: Moving towards cell culture-based viral vaccines. *Expert Review of Vaccines*, 8(5), 607–618.
- Bauer, D. E., Canver, M. C., & Orkin, S. H. (2015). Generation of genomic deletions in mammalian cell lines via CRISPR/Cas9. *Journal of Visualized Experiments: JoVE*, 95, e52118. <https://doi.org/10.3791/52118>
- Bunnik, E. M., & Le Roch, K. G. (2013). An introduction to functional genomics and systems biology. *Adv Wound Care (New Rochelle)*, 2(9), 490–498. <https://doi.org/10.1089/wound.2012.0379>
- Concordet, J. P., & Haeussler, M. (2018). CRISPOR: Intuitive guide selection for CRISPR/Cas9 genome editing experiments and screens. *Nucleic Acids Research*, 46(W1), W242–W245. <https://doi.org/10.1093/nar/gky354>
- Croft, D., Mundo, A. F., Haw, R., Milacic, M., Weiser, J., Wu, G., Caudy, M., Garapati, P., Gillespie, M., Kamdar, M. R., Jassal, B., Jupe, S., Matthews, L., May, B., Palatnik, S., Rothfels, K., Shamovsky, V., Song, H., Williams, M., ... D'Eustachio, P. (2014). The reactome pathway knowledgebase. *Nucleic Acids Research*, 42(Database issue), D472–D477. <https://doi.org/10.1093/nar/gkt1102>
- Dobin, A., Davis, C. A., Schlesinger, F., Drenkow, J., Zaleski, C., Jha, S., Batut, P., Chaisson, M., & Gingeras, T. R. (January 2013). STAR: Ultrafast universal RNA-seq aligner. *Bioinformatics* (Vol. 29, Issue 1 pp. 15–21). STAR: Ultrafast universal RNA-seq aligner.
- Dzimianski, J. V., Scholte, F. E. M., Bergeron, E., & Pegan, S. D. (2019). ISG15: It's complicated. *Journal of Molecular Biology*, 431(21), 4203–4216. <https://doi.org/10.1016/j.jmb.2019.03.013>
- Frensing, T., Kupke, S. Y., Bachmann, M., Fritzsche, S., Gallo-Ramirez, L. E., & Reichl, U. (2016). Influenza virus intracellular replication dynamics, release kinetics, and particle morphology during propagation in MDCK cells. *Applied Microbiology and Biotechnology*, 100(16), 7181–7192. <https://doi.org/10.1007/s00253-016-7542-4>
- Fulfer, J. P. C., Farnós, O., Kiesslich, S., Yang, Z., Dash, S., Susta, L., Wootton, S. K., & Kamen, A. A. (2021). Process development for newcastle disease Virus-Vectorized vaccines in Serum-Free vero cell suspension cultures. *Vaccines (Basel)*, 9(11), 1335. <https://doi.org/10.3390/vaccines9111335>
- Guillin, O. M., Vindry, C., Ohlmann, T., & Chavatte, L. (2019). Selenium, selenoproteins and viral infection. *Nutrients*, 11(9), 2101. <https://doi.org/10.3390/nu11092101>
- Harris, M. A., Clark, J., Ireland, A., Lomax, J., Ashburner, M., Foulger, R., Eilbeck, K., Lewis, S., Marshall, B., Mungall, C., Richter, J., Rubin, G. M., Blake, J. A., Bult, C., Dolan, M., Drabkin, H., Eppig, J. T., Hill, D. P., Ni, L., White, R., ... Gene Ontology Consortium. (2004). The Gene Ontology (GO) database and informatics resource. *Nucleic Acids Research*, 32(Database issue), D258–D261. <https://doi.org/10.1093/nar/gkh036>
- Hoeksema, F., Karpilow, J., Luitjens, A., Lagerwerf, F., Havenga, M., Groothuizen, M., Gillissen, G., Lemckert, A., Jiang, B., Tripp, R. A., & Yallop, C. (2018). Enhancing viral vaccine production using engineered knockout vero cell lines—A second look. *Vaccine*, 36(16), 2093–2103. <https://doi.org/10.1016/j.vaccine.2018.03.010>
- Hoffmann, M., Kleine-Weber, H., Schroeder, S., Krüger, N., Herrler, T., Erichsen, S., Schiergens, T. S., Herrler, G., Wu, N.-H., Nitsche, A., Müller, M. A., Drosten, C., & Pöhlmann, S. (2020). SARS-CoV-2 cell entry depends on ACE2 and TMPRSS2 and is blocked by a clinically proven protease inhibitor. *Cell*, S0092-8674(20), 30229–4.
- Kiesslich, S., Vila-Chã Losa, J. P., Gélinas, J. F., & Kamen, A. A. (2020). Serum-free production of rVSV-ZEBOV in Vero cells: Microcarrier bioreactor versus scale-X™ hydro fixed-bed. *Journal of Biotechnology*, 310, 32–39. <https://doi.org/10.1016/j.jbiotec.2020.01.015>
- Li, H., Handsaker, B., Wysoker, A., Fennell, T., Ruan, J., Homer, N., Marth, G., Abecasis, G., Durbin, R., & Genome Project Data Processing, S. (2009). The sequence Alignment/Map format and SAMtools. *Bioinformatics (Oxford, England)*, 25(16), 2078–2079.
- Liao, Y., Smyth, G. K., & Shi, W. (2014). featureCounts: An efficient general purpose program for assigning sequence reads to genomic features. *Bioinformatics*, 30(7), 1.
- Liao, Y., Wang, J., Jaehning, E. J., Shi, Z., & Zhang, B., WebGestalt. (2019). Gene set analysis toolkit with revamped UIs and APIs. *Nucleic Acids Research*, 47(W1), W199–W205.
- Liu, R., Wang, J., Shao, Y., Wang, X., Zhang, H., Shuai, L., Ge, J., Wen, Z., & Bu, Z. (2018). A recombinant VSV-vectored MERS-CoV vaccine induces neutralizing antibody and T cell responses in rhesus monkeys after single dose immunization. *Antiviral Research*, 150, 30–38.
- Love, M. I., Huber, W., & Anders, S. (2014). Moderated estimation of fold change and dispersion for RNA-seq data with DESeq2. *Genome Biology*, 15, 550. <https://doi.org/10.1186/s13059-014-0550-8>
- Orr-Burks, N., Murray, J., Wu, W., et al. (2019). Gene-edited vero cells as rotavirus vaccine substrates. *Published Vaccine X*. 2019;3:100045 Oct 8 <https://doi.org/10.1016/j.jvaxc.2019.100045>
- Pattyn, E., Verhee, A., Uyttendaele, I., Piessevaux, J., Timmerman, E., Gevaert, K., Vandekerckhove, J., Peelman, F., & Tavernier, J. (2008). HyperISGylation of Old World monkey ISG15 in human cells. *PLoS One*, 3(6), e2427. <https://doi.org/10.1371/journal.pone.0002427>
- Peng, D., & Tarleton, R. (2015). EuPaGDT: A web tool tailored to design CRISPR guide RNAs for eukaryotic pathogens. *Microbial Genomics*, 1(4), e000033. <https://doi.org/10.1099/mgen.0.000033>
- Perng, Y. C., & Lenschow, D. J. (2018). ISG15 in antiviral immunity and beyond. *Nature Reviews Microbiology*, 16(7), 423–439. <https://doi.org/10.1038/s41579-018-0020-5>
- Popp, M. W., Cho, H., & Maquat, L. E. (2020). Viral subversion of nonsense-mediated mRNA decay. *RNA*, 26(11), 1509–1518. <https://doi.org/10.1261/rna.076687.120>
- Robert, X., & Gouet, P. (2014). Deciphering key features in protein structures with the new ENDscript server. *Nucleic Acids Research*, 42(Web Server issue), W320–W324. <https://doi.org/10.1093/nar/gku316>
- Van der Sanden, S. M., Wu, W., Dybdahl-Sissoko, N., Weldon, W. C., Brooks, P., O'Donnell, J., Jones, L. P., Brown, C., Tompkins, S. M., Oberste, M. S., Karpilow, J., & Tripp, R. A. (2016). Engineering enhanced vaccine cell lines to eradicate Vaccine-Preventable Diseases: The Polio End Game. *Journal of Virology*, 90(4), 1694–1704.
- Sascha Kiesslich, A. A. (2020). Kamen, Vero cell upstream bioprocess development for the production of viral vectors and vaccines. *Biotechnology Advances*, 44, 107608, ISSN 0734-9750
- Sène, M. A., Kiesslich, S., Djambazian, H., Ragoussis, J., Xia, Y., & Kamen, A. A. (2021). Haplotype-resolved de novo assembly of the Vero cell line genome. *NPJ Vaccines*, 6(1), 106. <https://doi.org/10.1038/s41541-021-00358-9> PMID: 344 17462
- Speer, S., Li, Z., Buta, S., Payelle-Brogard, B., Qian, L., Vigant, F., Rubino, E., Gardner, T., Wedeking, T., Hermann, M., Duehr, J., Sanal, O., Tezcan, i., Mansouri, N., Tabarsi, P., Mansouri, D., Francois-Newton, V., Daussy, C., Rodriguez, M., & Bogunovic, D. (2016). ISG15 deficiency and increased

- viral resistance in humans but not mice. *Nature Communications*, 7, 11496. <https://doi.org/10.1038/ncomms11496>
- Stark, C., Breitkreutz, B. J., Reguly, T., Boucher, L., Breitkreutz, A., & Tyers, M. (2006). BioGRID: A general repository for interaction datasets. *Nucleic Acids Research*, 34, D535–D539.
- Suder, E., Furuyama, W., Feldmann, H., Marzi, A., & de Wit, E. (2018). The vesicular stomatitis virus-based Ebola virus vaccine: From concept to clinical trials. *Human Vaccines & Immunotherapeutics*, 14(9), 2107–2113.
- Di Tommaso, P., Moretti, S., Xenarios, I., Oorbitg, M., Montanyola, A., Chang, J. M., Taly, J. F., & Notredame, C. (2011). T-Coffee: A web server for the multiple sequence alignment of protein and RNA sequences using structural information and homology extension. *Nucleic Acids Research*, 39(Web Server issue), W13–W17. <https://doi.org/10.1093/nar/gkr245>
- Wang, J., Ma, Z., Carr, S. A., Mertins, P., Zhang, H., Zhang, Z., Chan, D. W., Ellis, M. J., Townsend, R. R., Smith, R. D., McDermott, J. E., Chen, X., Paulovich, A. G., Boja, E. S., Mesri, M., Kinsinger, C. R., Rodriguez, H., Rodland, K. D., Liebler, D. C., & Zhang, B. (2017). Proteome profiling outperforms transcriptome profiling for coexpression based gene function prediction. *Molecular & Cellular Proteomics*, 16(1), 121–134. <https://doi.org/10.1074/mcp.M116.060301>
- WHO. (2022). COVID-19 vaccine tracker and landscape. <https://www.who.int/teams/blueprint/covid-19/covid-19-vaccine-tracker-and-landscape>

SUPPORTING INFORMATION

Additional supporting information can be found online in the Supporting Information section at the end of this article.

How to cite this article: Sène, M.-A., Xia, Y., & Kamen, A. A. (2022). From Functional Genomics of Vero cells to CRISPR-based Genomic deletion for improved viral production rates. *Biotechnology and Bioengineering*, 119, 2794–2805. <https://doi.org/10.1002/bit.28190>